

Two High-Performance Amplitude Beamforming Schemes for Secure Precise Communication and Jamming with Phase Alignment

Lingling Zhu¹, Feng Shu¹, and Tong Shen¹

¹School of Electronic and Optical Engineering, Nanjing University of Science and Technology, Nanjing, China
Emails: {zhulingling@njust.edu.cn, shufeng@njust.edu.cn, shentong0107@163.com}

Abstract—To severely weaken the eavesdropper’s ability to intercept confidential message (CM), a precise jamming (PJ) idea is proposed by making use of the concept of secure precise wireless transmission (SPWT). Its basic idea is to focus the transmit energy of artificial noise (AN) onto the neighborhood of eavesdropper (Eve) by using random subcarrier selection (RSS), directional modulation, phase alignment (PA), and amplitude beamforming (AB). By doing so, Eve will be seriously interfered with AN. Here, the conventional joint optimization of phase and amplitude is converted into two independent phase and amplitude optimization problems. Considering PJ and SPWT require PA, the joint optimization problem reduces to an amplitude optimization problem. Then, two efficient AB schemes are proposed: leakage and maximizing receive power (Max-RP). With existing equal AB (EAB) as a performance reference, simulation results show that the proposed Max-RP and leakage AB methods perform much better than conventional method in terms of both bit-error-rate (BER) and secrecy rate (SR) at medium and high signal-to-noise ratio regions. The performance difference between the two proposed leakage and Max-RP amplitude beamformers is trivial. Additionally, we also find the fact that all three AB schemes EA, Max-RP, and leakage can form two main peaks of AN and CM around Eve and the desired receiver (Bob), respectively. This is what we call PJ and SPWT.

Index Terms—Secure precise wireless transmission, precise jamming, phase alignment, secrecy rate, bit error rate.

I. INTRODUCTION

In recent years, physical-layer security (PLS) has become a promising research field both in academia and industry [1]–[5]. Various tools can be used to achieve PLS, including code, modulations and relay cooperation, etc. Secure spatial modulation is proposed to achieve a secure transmission in fading channel. Its basic technology consists of transmit antenna selection, beamforming of confidential message (CM), and artificial noise (AN) projection [6]–[8]. As a PLS technology, directional modulation (DM) [9] has attracted recently substantial research activities directly applied to millimeter wave and UAV channels, which provides an alternative secure solution for the future wireless networks. To achieve secure transmission, maximum group receive power (Max-GRP) and leakage methods in [10] are proposed for multi-cast multiuser DM system.

Inspired by DM, the authors in [11], [12] proposed secure precise wireless transmission (SPWT) based on DM. Its basic idea is to use frequency diverse array (FDA) as a potential

solution to solve the security problem of DM (i.e., rely solely on direction angle). FDA [13] employs different frequency offsets to decouple the channels of Bob and Eve. In other words, the range-angle-dependent characteristic is established and there is a single main peak of CM is formed around Bob. In [14], the authors optimize the frequency offsets by block successive upper-bound minimization algorithm to ensure the maximum secrecy rate (SR) of proximal Bob and Eve scenario. However, consider that Eve is sensitive enough, the authors in [15] added artificial noise (AN) to the proximal Bob and Eve scenario to cause interferences to the Eve, and extended the frequency offset optimization in the case of multiple eavesdroppers. The authors in [12] proposed a new SPWT transmit structure. Random subcarrier selection (RSS) of orthogonal frequency diversion multiplexing (OFDM) is applied to reduce the complexity of SPWT receiver. To achieve a SPWT per OFDM symbol, two practical RSS methods by randomization procedure including integer mod, ordering, and block interleaving [16].

Although beamforming schemes have been investigated intensively, almost all of the previous studies design the amplitude and phase simultaneously. In this letter, we propose a novel beamforming scheme for a communication system of PJ with artificial noise based on random-subcarrier-selection (RSS-PJ-AN), our main contributions in this paper are as follows:

- 1) To focus the AN energy on Eve, we extend the idea of SPWT to a precise jamming (PJ). By doing so, Eve will be degraded seriously. To achieve both SPWT and PJ, phase alignment (PA) is mandatory for the beamforming vectors of CM and AN. Then, a novel beamforming framework is proposed for SPWT and PJ. In other words, the beamforming design is decomposed into two parts: PA and amplitude beamforming (AB).
- 2) Using the proposed new beamforming framework, two AB schemes are proposed: leakage and maximum receive power (Max-RP). Both AB of AN and CM are based on the two rules. Simulation results show that, compared to equal AB (EAB), the proposed two AB schemes leakage and Max-RP perform better in the medium and high signal-to-noise ratio (SNR) regions in

terms of SR and bit-error-rate (BER) performance while they have the same performance as EAB in the low SNR region.

The remainder of this letter is organized as follows. In Section II, we describe RSS-PJ-AN system model. Subsequently, we propose two AB methods: leakage-based and Max-RP in Section III. In Section IV, the performance of the proposed scheme is numerically evaluated, and conclusions are given in Section V.

Notations: matrices, vectors, and scalars are denoted by letters of bold upper case, bold lower case, and lower case, respectively. Signs $(\cdot)^T$, $(\cdot)^H$ and $(\cdot)^{-1}$ denote matrix transpose, conjugate transpose and Moore-Penrose inverse, respectively. The operation $|\cdot|$ denotes modulus of a complex number. The symbol \mathbf{I}_N denotes the $N \times N$ identity matrix.

II. SYSTEM MODEL

Fig. 1 illustrates a typical architecture for RSS-PJ-AN system model consisting of an N -antenna uniform linear transmit array, a single-antenna Bob and a single-antenna Eve. CM is transmitted towards Bob via randomly-selected multiple subcarriers from all-subcarrier set of OFDM. The all-subcarrier set of OFDM is $S_{sub} = \{f_m | f_m = f_c + m\Delta f, m = 0, 1, \dots, N_S - 1\}$, where f_c is the carrier frequency and Δf is the subchannel bandwidth. The subcarrier assigned to n -th antenna is f_n , where $f_n \in S_{sub}$ [12].

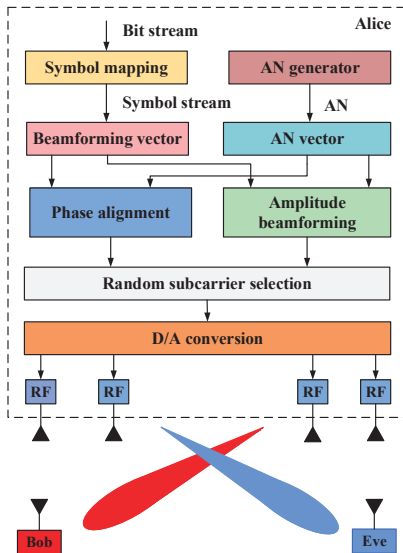


Fig. 1. Block diagram for RSS-PJ-AN systems.

In this work, we assume that the channels between transmitter and receivers are LoP ones. The normalized steering vector for the transmit antenna array is given by

$$\mathbf{h}(\theta, R) = \frac{1}{\sqrt{N}} [e^{j\Psi_0(\theta, R)}, \dots, e^{j\Psi_{N-1}(\theta, R)}]^T, \quad (1)$$

where $\Psi_n(\theta, R) = 2\pi(f_c + k_n\Delta f) \frac{R - (n-1)d \cos \theta}{c} - 2\pi f_c \frac{R}{c}$ with d being element spacing of uniform linear array (ULA) and c being light speed. θ and R are the direction angle and

distance from Alice to receiver. Normally, frequency increment and central carrier frequency can satisfy $N_S \Delta f \ll f_c$. It is assumed that Bob and Eve are located at (θ_B, R_B) and (θ_E, R_E) with a high-resolution direction of arrival estimation [17], respectively.

The baseband transmit signal can be expressed as

$$\mathbf{s} = \sqrt{\beta P_s} \mathbf{v}_{CM} x + \sqrt{(1 - \beta) P_s} \mathbf{v}_{AN} z, \quad (2)$$

where x is the CM and z is the AN both with average power constraint (i.e., $E[|x|^2] = 1$, $E[|z|^2] = 1$). P_s is the transmit power of Alice and β is the parameter that determines the power allocation between the CM and AN. \mathbf{v}_{CM} and \mathbf{v}_{AN} are the normalized CM beamforming vector and the normalized AN vector, respectively.

Considering that SPWT and PJ require \mathbf{v}_{CM} to align with Bob (θ_B, R_B) and \mathbf{v}_{AN} to align with Eve (θ_E, R_E) , the n -th element of phase vector of \mathbf{v}_{CM} and \mathbf{v}_{AN} can be expressed as $\arg(\mathbf{v}_{CM}(n)) = \Psi_n(\theta_B, R_B)$ and $\arg(\mathbf{v}_{AN}(n)) = \Psi_n(\theta_E, R_E)$, respectively. Here, we define $\mathbf{v}_{CM} = \mathbf{P}\mathbf{a}$ and $\mathbf{v}_{AN} = \mathbf{Q}\mathbf{b}$, where \mathbf{P} and \mathbf{Q} are both diagonal matrix as $\mathbf{P} = \text{diag}[\arg(\mathbf{v}_{CM}(0)), \dots, \arg(\mathbf{v}_{CM}(N-1))]$ and $\mathbf{Q} = \text{diag}[\arg(\mathbf{v}_{AN}(0)), \dots, \arg(\mathbf{v}_{AN}(N-1))]$, respectively. $\mathbf{P}(n, n)$ and $\mathbf{Q}(n, n)$ represent the n -th element phases of \mathbf{v}_{CM} and \mathbf{v}_{AN} , respectively. Meanwhile, \mathbf{a} is the AB vector of \mathbf{v}_{CM} and \mathbf{b} is the AB vector \mathbf{v}_{AN} (i.e., $|\mathbf{v}_{CM}(n)| = |\mathbf{a}(n)|$ and $|\mathbf{v}_{AN}(n)| = |\mathbf{b}(n)|$).

Accordingly, the received signal at Bob and Eve can be formulated as follows

$$y(\theta_B, R_B) = \sqrt{g_d \beta P_s} \mathbf{h}^H(\theta_B, R_B) \mathbf{P} \mathbf{a} x + \sqrt{g_d (1 - \beta) P_s} \mathbf{h}^H(\theta_B, R_B) \mathbf{Q} \mathbf{b} z + n_B, \quad (3)$$

and

$$y(\theta_E, R_E) = \sqrt{g_e \beta P_s} \mathbf{h}^H(\theta_E, R_E) \mathbf{P} \mathbf{a} x + \sqrt{g_e (1 - \beta) P_s} \mathbf{h}^H(\theta_E, R_E) \mathbf{Q} \mathbf{b} z + n_E, \quad (4)$$

where n_B and n_E are the additive white Gaussian noise (AWGN), distributed as $n \sim \mathcal{CN}(0, \sigma_B^2)$ and $n \sim \mathcal{CN}(0, \sigma_E^2)$, respectively. $g_d = R_0/R_B^2$ and $g_e = R_0/R_E^2$ denote path loss coefficients from Alice to Bob and from Alice to Eve, respectively. R_0 is the reference distance which is set to 1m.

In what follows, for the convenience of optimization, \mathbf{a} and \mathbf{b} is relaxed as complex optimization variables, and the corresponding element magnitudes of vectors \mathbf{v}_{CM} and \mathbf{v}_{AN} are set to be the element magnitudes of optimal \mathbf{a} and \mathbf{b} in terms of some rules.

III. TWO PROPOSED AB SCHEMES

In this section, to improve the SR performance, two AB schemes leakage and Max-RP with EAB methods are proposed to optimize the amplitude parts of the beamforming vectors of AN and CM. Here, their phase parts is directly set to the negation of phases of channel steering vectors in order to form the main peaks of CM and AN at Bob and Eve, respectively.

A. Proposed Leakage-Based AB Method

Making use of leakage criterion, we use the maximizing signal-to-leakage-noise ratio (Max-SLNR) method to optimize the vector \mathbf{a} , which can be obtained as

$$\begin{aligned} \max_{\mathbf{a}} \quad & \text{SLNR}(\mathbf{a}) \\ \text{s.t.} \quad & \mathbf{a}^H \mathbf{a} = 1, \end{aligned} \quad (5)$$

where

$$\text{SLNR}(\mathbf{a}) = \frac{g_d \mathbf{a}^H \mathbf{P}^H \mathbf{h}(\theta_B, R_B) \mathbf{h}^H(\theta_B, R_B) \mathbf{P} \mathbf{a}}{\mathbf{a}^H (g_e \mathbf{P}^H \mathbf{h}(\theta_E, R_E) \mathbf{h}^H(\theta_E, R_E) \mathbf{P} + \frac{\sigma^2}{\beta P_s} \mathbf{I}_N) \mathbf{a}}. \quad (6)$$

which yields the vector \mathbf{a} being the eigenvector corresponding to the largest eigenvalue of matrix

$$\begin{bmatrix} g_e \mathbf{P}^H \mathbf{h}(\theta_E, R_E) \mathbf{h}^H(\theta_E, R_E) \mathbf{P} + \frac{\sigma^2}{\beta P_s} \mathbf{I}_N \end{bmatrix}^{-1} \times g_d \mathbf{P}^H \mathbf{h}(\theta_B, R_B) \mathbf{h}^H(\theta_B, R_B) \mathbf{P}. \quad (7)$$

Since \mathbf{a} is a complex vector. The magnitude $|\mathbf{v}_{CM}(n)|$ of element n of vector is chosen to be $|\mathbf{a}(n)|$. Next, the AN is viewed as the useful signal of Eve. Let \mathbf{b} be the optimization vector, similarly, we have

$$\begin{aligned} \max_{\mathbf{b}} \quad & \text{SLNR}(\mathbf{b}) \\ \text{s.t.} \quad & \mathbf{b}^H \mathbf{b} = 1, \end{aligned} \quad (8)$$

where

$$\text{SLNR}(\mathbf{b}) = \frac{g_e \mathbf{b}^H \mathbf{Q}^H \mathbf{h}(\theta_B, R_B) \mathbf{h}^H(\theta_B, R_B) \mathbf{Q} \mathbf{b}}{\mathbf{b}^H (g_d \mathbf{Q}^H \mathbf{h}(\theta_E, R_E) \mathbf{h}^H(\theta_E, R_E) \mathbf{Q} + \frac{\sigma^2}{\beta P_s} \mathbf{I}_N) \mathbf{b}}. \quad (9)$$

which results in the optimal value of \mathbf{b} being the generalized eigenvector corresponding to the largest normalized eigenvalue of matrix

$$\begin{bmatrix} g_d \mathbf{Q}^H \mathbf{h}(\theta_B, R_B) \mathbf{h}^H(\theta_B, R_B) \mathbf{Q} + \frac{\sigma^2}{(1-\beta) P_s} \mathbf{I}_N \end{bmatrix}^{-1} \times g_e \mathbf{Q}^H \mathbf{h}(\theta_E, R_E) \mathbf{h}^H(\theta_E, R_E) \mathbf{Q}. \quad (10)$$

Likewise, the AB vector of \mathbf{v}_{AN} is taken to be $[\mathbf{b}(0), |\mathbf{b}(1)|, \dots, |\mathbf{b}(N-1)|]^T$.

B. Proposed Max-RP-based AB Method

Now, we turn to a new rule. By maximizing the receive power of CM at Bob, the AB part of \mathbf{v}_{CM} are constructed. The corresponding optimization problem of Max-RP is given by

$$\begin{aligned} \max_{\mathbf{a}} \quad & \mathbf{a}^H \mathbf{P}^H \mathbf{h}(\theta_B, R_B) \mathbf{h}^H(\theta_B, R_B) \mathbf{P} \mathbf{a} \\ \text{s.t.} \quad & \mathbf{h}^H(\theta_E, R_E) \mathbf{P} \mathbf{a} = 0. \end{aligned} \quad (11)$$

where the constraint $\mathbf{h}^H(\theta_E, R_E) \mathbf{P} \mathbf{a} = 0$ forces CM to transmit on the null space of $\mathbf{h}^H(\theta_E, R_E) \mathbf{P}$. To address the above problem, the singular-value decomposition (SVD) of $\mathbf{h}^H(\theta_E, R_E) \mathbf{P}$ is computed as $\mathbf{h}^H(\theta_E, R_E) \mathbf{P} = [U_e] (\sum_e^{(1)} \mathbf{0}) [\mathbf{V}_e^{(1)} \mathbf{V}_e^{(0)}]^H$, where $\sum_e^{(1)}$ is a complex number, and $\mathbf{V}_e^{(0)}$ consists of the last $(N-1)$ right singular

vectors corresponding to $N-1$ zero singular values. Define $\mathbf{F}_e = \mathbf{V}_e^{(0)}$, and $\mathbf{a} = \mathbf{F}_e \mathbf{u}$, then the optimization problem in (11) is converted into

$$\begin{aligned} \max_{\mathbf{u}} \quad & \mathbf{u}^H \mathbf{F}_e^H \mathbf{P}^H \mathbf{h}(\theta_B, R_B) \mathbf{h}^H(\theta_B, R_B) \mathbf{P} \mathbf{F}_e \mathbf{u} \\ \text{s.t.} \quad & \mathbf{u}^H \mathbf{u} = 1, \end{aligned} \quad (12)$$

which means that \mathbf{u} is the eigenvector corresponding to the largest eigenvalue of matrix $\mathbf{F}_e^H \mathbf{P}^H \mathbf{h}(\theta_B, R_B) \mathbf{h}^H(\theta_B, R_B) \mathbf{P} \mathbf{F}_e$. The design of \mathbf{a} has been finished. Then, the AB vector of \mathbf{v}_{CM} is $[\mathbf{a}(0), \dots, |\mathbf{a}(N-1)|]^T$.

Similar to (11), we can readily obtain

$$\begin{aligned} \max_{\mathbf{b}} \quad & \mathbf{b}^H \mathbf{Q}^H \mathbf{h}(\theta_E, R_E) \mathbf{h}^H(\theta_E, R_E) \mathbf{Q} \mathbf{b} \\ \text{s.t.} \quad & \mathbf{h}^H(\theta_B, R_B) \mathbf{Q} \mathbf{b} = 0. \end{aligned} \quad (13)$$

The SVD of $\mathbf{h}^H(\theta_B, R_B) \mathbf{Q}$ is $\mathbf{h}^H(\theta_B, R_B) \mathbf{Q} = [U_b] (\sum_b^{(1)} \mathbf{0}) [\mathbf{V}_b^{(1)} \mathbf{V}_b^{(0)}]^H$. Define $\mathbf{F}_b = \mathbf{V}_b^{(0)}$, and $\mathbf{b} = \mathbf{F}_b \mathbf{w}$, then the optimization problem in (13) can also be expressed as

$$\begin{aligned} \max_{\mathbf{w}} \quad & \mathbf{w}^H \mathbf{F}_b^H \mathbf{Q}^H \mathbf{h}(\theta_E, R_E) \mathbf{h}^H(\theta_E, R_E) \mathbf{Q} \mathbf{F}_b \mathbf{w} \\ \text{s.t.} \quad & \mathbf{w}^H \mathbf{w} = 1, \end{aligned} \quad (14)$$

where \mathbf{w} is the eigenvector corresponding to the largest eigenvalue of matrix $\mathbf{F}_b^H \mathbf{Q}^H \mathbf{h}(\theta_E, R_E) \mathbf{h}^H(\theta_E, R_E) \mathbf{Q} \mathbf{F}_b$. Then the design of \mathbf{b} and $|\mathbf{v}_{AN}(n)| = |\mathbf{b}(n)|$ have been completed.

IV. SIMULATIONS AND DISCUSSIONS

In our simulation, system parameters are set as follows: quadrature phase shift keying (QPSK) modulation, the total signal bandwidth is 5MHz, $f_c = 3\text{GHz}$, the number of total subcarriers $N_S = 1024$, $N = 32$, $d = \lambda/2$, $\beta = 0.5$, $\sigma_B^2 = \sigma_E^2 = -60\text{dBm}$, $(\theta_B, R_B) = (30^\circ, 650\text{m})$ and $(\theta_E, R_E) = (100^\circ, 550\text{m})$.

Fig. 2 plots the three-dimensional (3D) performance surface of signal-to-interference-plus-noise ratio (SINR) versus direction angle θ and distance R of proposed methods for SNR = 14dB, where the conventional EAB method is used as a performance reference. Here, CM is a useful signal for Bob, and AN is a useful signal for Eve. Observing three parts in Fig. 2, two peaks of CM and AN are only around Bob ($30^\circ, 650\text{m}$) and Eve ($100^\circ, 550\text{m}$), respectively. Additionally, we also find a fact that the main peaks of Bob and Eve of the proposed methods are much higher than those of EAB, which means that the proposed methods have a better SINR performance.

Fig. 3 shows the curves of BER versus the SNR, for the two proposed AB schemes described in Section-III. The figure illustrates that our proposed methods outperform the EAB. Particularly in the high SNR region, the BER performance of our proposed schemes is about one order of magnitude, better than that of the EAB method.

In what follows, we also evaluate the performance of the proposed AB schemes from SR [1] aspect. Fig. 4 demonstrates the curves of SR versus SNR of the proposed AB methods.

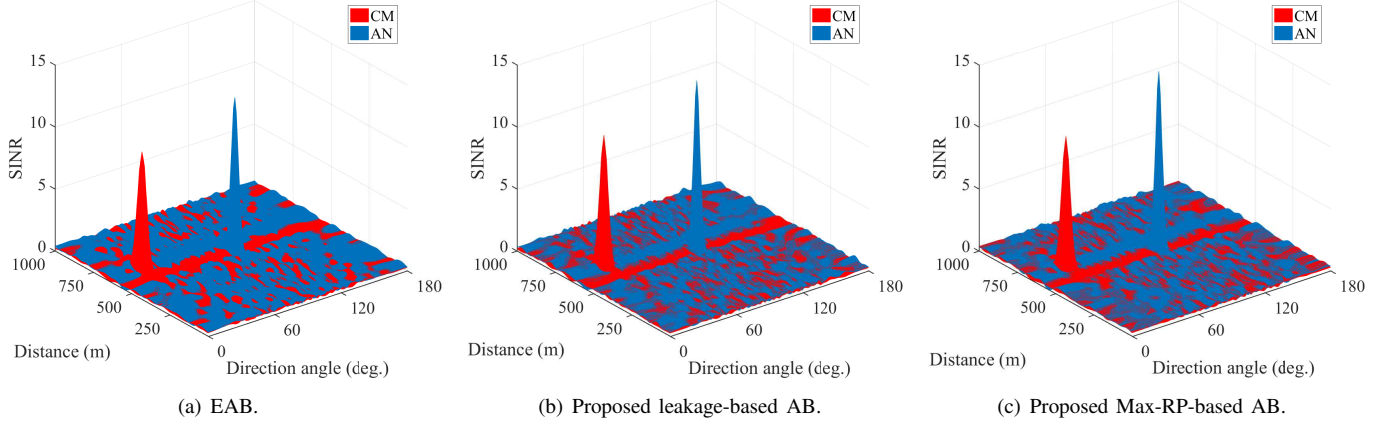


Fig. 2. 3D surface of SINR versus direction angle and distance of EAB, proposed leakage-based AB and proposed Max-RP-based AB.

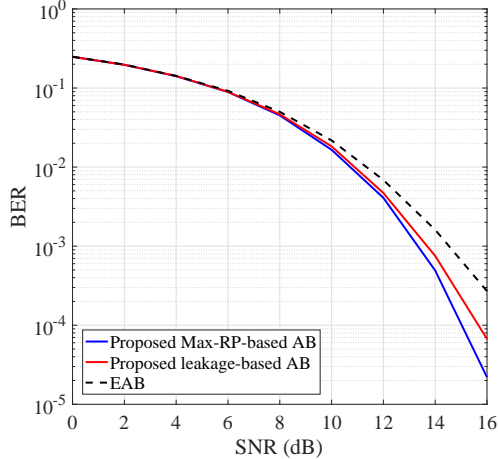


Fig. 3. Curves of BER with EAB, proposed leakage-based AB and proposed Max-RP-based AB versus SNR.

From Fig. 4, it is noted that the SR performance of the three method are close to each other in the low SNR region. As SNR grows, the performance gap between the proposed schemes and EAB method becomes larger, which greatly improves the security of communication system.

V. CONCLUSION

In this paper, we mainly proposed two high-performance AB methods: leakage and Max-RP to enhance the physical layer security of wireless communication. Simulation results showed that our proposed two AB methods behave better than EAB method in terms of BER and SR.

VI. ACKNOWLEDGMENT

This work was supported in part by the National Natural Science Foundation of China (Nos. 61771244, 61501238, 61702258, 61472190, and 61271230).

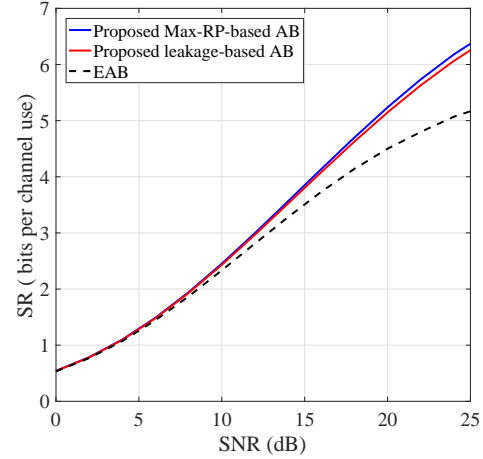


Fig. 4. Curves of SR with EAB, proposed leakage-based AB and proposed Max-RP-based AB versus SNR.

REFERENCES

- [1] A. D. Wyner, "The wire-tap channel," *Bell. Syst. Tech. J.*, vol. 54, no. 8, pp. 1355–1387, Oct. 1975.
- [2] J. Guo, N. Zhao, F. R. Yu, X. Liu, and V. C. M. Leung, "Exploiting adversarial jamming signals for energy harvesting in interference networks," *IEEE Trans. Wireless Commun.*, vol. 16, no. 2, pp. 1267–1280, Feb 2017.
- [3] X. Chen, D. W. K. Ng, W. H. Gerstacker, and H. Chen, "A survey on multiple-antenna techniques for physical layer security," *IEEE Commun. Surv. Tut.*, vol. 19, no. 2, pp. 1027–1053, Secondquarter 2017.
- [4] Y. Wu, J. Wang, J. Wang, R. Schober, and C. Xiao, "Secure transmission with large numbers of antennas and finite alphabet inputs," *IEEE Trans. Commun.*, vol. 65, no. 8, pp. 3614–3628, Aug 2017.
- [5] J. Ma, S. Zhang, H. Li, N. Zhao, and V. C. M. Leung, "Interference-alignment and soft-space-reuse based cooperative transmission for multi-cell massive mimo networks," *IEEE Trans. Wireless Commun.*, vol. 17, no. 3, pp. 1907–1922, March 2018.
- [6] F. Shu, Z. Wang, R. Chen, Y. Wu, and J. Wang, "Two high-performance schemes of transmit antenna selection for secure spatial modulation," *IEEE Trans. Veh. Technol.*, vol. 67, no. 9, pp. 8969–8973, Sep. 2018.
- [7] G. Xia, F. Shu, Y. Zhang, J. Wang, S. ten Brink, and J. Speidel, "Antenna selection method of maximizing secrecy rate for green secure spatial modulation," *IEEE Trans. Green Commun. Netw.*, vol. 3, no. 2, pp. 288–301, Jun. 2019.

- [8] X. Yu, Y. Hu, Q. Pan, X. Dang, N. Li, and M. H. Shan, "Secrecy performance analysis of artificial-noise-aided spatial modulation in the presence of imperfect csi," *IEEE Access*, vol. 6, pp. 41 060–41 067, 2018.
- [9] Y. Ding and V. F. Fusco, "A vector approach for the analysis and synthesis of directional modulation transmitters," *IEEE Trans. Antennas Propag.*, vol. 62, no. 1, pp. 361–370, Jan 2014.
- [10] F. Shu, L. Xu, J. Wang, W. Zhu, and Z. Xiaobo, "Artificial-noise-aided secure multicast precoding for directional modulation systems," *IEEE Trans. Veh. Technol.*, vol. 67, no. 7, pp. 6658–6662, July 2018.
- [11] J. Hu, S. Yan, F. Shu, J. Wang, J. Li, and Y. Zhang, "Artificial-noise-aided secure transmission with directional modulation based on random frequency diverse arrays," *IEEE Access*, vol. 5, pp. 1658–1667, 2017.
- [12] F. Shu, X. Wu, J. Hu, J. Li, R. Chen, and J. Wang, "Secure and precise wireless transmission for random-subcarrier-selection-based directional modulation transmit antenna array," *IEEE J. Sel. Areas Commun.*, vol. 36, no. 4, pp. 890–904, April 2018.
- [13] P. Antonik, M. C. Wicks, H. D. Griffiths, and C. J. Baker, "Frequency diverse array radars," in *2006 IEEE Radar Conf.*, Apr. 2006, pp. 3 pp.–.
- [14] J. Lin, Q. Li, J. Yang, H. Shao, and W. Wang, "Physical-layer security for proximal legitimate user and eavesdropper: A frequency diverse array beamforming approach," *IEEE Trans. Inf. Forensics Security*, vol. 13, no. 3, pp. 671–684, Mar. 2018.
- [15] B. Qiu, J. Xie, L. Wang, and Y. Wang, "Artificial-noise-aided secure transmission for proximal legitimate user and eavesdropper based on frequency diverse arrays," *IEEE Access*, vol. 6, pp. 52 531–52 543, 2018.
- [16] T. Shen, S. Zhang, J. Wang, J. Hu, F. Shu, and J. Wang, "Two practical random-subcarrier-selection methods for secure precise wireless transmissions," *IEEE Trans. Veh. Technol.*, pp. 1–1, 2019.
- [17] F. Shu, Y. Qin, T. Liu, L. Gui, Y. Zhang, J. Li, and Z. Han, "Low-complexity and high-resolution doa estimation for hybrid analog and digital massive mimo receive array," *IEEE Trans. Commun.*, vol. 66, no. 6, pp. 2487–2501, Jun. 2018.